11A.3 **THE IMPACT OF DROPSONDE DATA FROM DOTSTAR ON TROPICAL CYCLONE TRACK FORECASTING**

Kun-Hsuan Chou[1], Chun-Chieh Wu[1, *] and Po-Hsiung Lin[1], Sim Aberson[2], Melinda Peng[3], Tetsuo Nakazawa[4]

[1]Dept. of Atmospheric Sciences, National Taiwan University, Taipei, Taiwan

[2]Hurricane Research Division, NOAA/AOML, Miami, Florida, USA

[3]Marine Meteorology Division, Naval Research Laboratory, Monterey, CA

[4]Meteorological Research Institute, Japan Meteorological Agency, Tokyo, Japan

**Abstract**

DOTSTAR, short for Dropwindsonde Observations for Typhoon Surveillance near the Taiwan Region, is an international research program conducted by meteorologists in Taiwan partnered with scientists at the Hurricane Research Division (HRD) and the National Centers for Environmental Prediction (NCEP) of the National Oceanic and Atmospheric Administration (NOAA). The DOTSTAR research team launched their typhoon surveillance in 2003. During 2004, 10 missions for 8 typhoons were conducted successfully with 155 dropwindsondes deployed. In this study, the impact of the dropwindsonde data on tropical cyclone track forecasts has been evaluated with five models (4 operational and 1 research).

All models, except the Geophysical Fluid Dynamics Laboratory (GFDL) hurricane model, show positive impact the dropwindsonde data have on tropical cyclone track forecasts. During the first 72 h, the mean track error reductions in the NCEP Global Forecast System (GFS), the Navy Operational Global Atmospheric Prediction System (NOGAPS) of the Fleet Numerical Meteorology and Oceanography Center (FNMOC) and the Japanese Meteorological Agency (JMA) Global Spectral Model (GSM), are 14, 14, and 19%, respectively. The track error reduction in the Weather Research and Forecasting (WRF) model, in which the initial conditions are directly interpolated from the operational GFS forecast, is 16%. However, the mean track improvement in the GFDL model is a statistically insignificant 3%. The 72-h average track error reduction from the ensemble mean of the above three global models is 22%, which is consistent with the track forecast improvement in Atlantic tropical cyclones from surveillance missions. In all, despite the limited number of DOTSTAR cases in 2004, the overall added value of the dropwindsonde data in improving typhoon track forecasts over the Northwestern Pacific is proven.

## 1. Introduction

Taiwan is severely affected by typhoons frequently, and the loss of life and property has been staggering. Prompted by the National Science Council's (NSC) sense of social responsibility and its emphasis on typhoon research, atmospheric scientists in Taiwan in July, 2002, initiated an interagency research project on typhoons, the “National Priority Typhoon Research Project.” One key part of this project involves a field experiment, Dropwindsonde Observations for Typhoon Surveillance near the Taiwan Region (DOTSTAR), marking the beginning of an era of tropical cyclones surveillance in the western North Pacific using GPS dropwindsondes. An overview of DOTSTAR is provided in Wu et al. (2005), and targeted observing strategies are discussed in Wu et al. (2006a). The detailed results of this work are also shown in Wu et al. (2006b).

DOTSTAR is a collaboration between researchers from the National Taiwan University (NTU) and the Central Weather Bureau (CWB), in partnership with scientists at the Hurricane Research Division (HRD) and the National Centers for Environmental Prediction (NCEP), both part of the National Oceanic and Atmospheric Administration (NOAA), built upon work pioneered by HRD to improve tropical cyclone track forecasts (Aberson 2003; see more detailed review in section 2). To make the maximum use of the DOTSTAR data, they are transmitted and assimilated in real time into the numerical models of CWB, NCEP, the U.S.

* *Corresponding author address*: Chun-Chieh Wu, Dept. of Atmospheric Sciences, National Taiwan University, No. 1, Sec. 4, Roosevelt Rd., Taipei, 106, Taiwan. E-mail: cwu@typhoon.as.ntu.edu.tw

Navy's Fleet Numerical Meteorology and Oceanography Center (FNMOC), and the Japanese Meteorological Agency (JMA).

With the experience gained from the successful first two surveillance flights for Typhoons Dujuan and Melor in 2003 (Wu et al. 2005), DOTSTAR conducted 10 more surveillance missions for Typhoons Nida, Conson, Mindulle, Megi, Aere, Meari, Nock-Ten, and Nanmadol in 2004 and released 155 dropwindsondes. The observation time, position and intensity of the observed tropical cyclones are summarized in Table 1, and the best tracks are shown in Fig. 1. The impact of the dropwindsonde data obtained during 2004 on global numerical models from three operational centers (NCEP, FNMOC, and JMA) is evaluated. The impact on two other regional models, i.e. the GFDL hurricane model (Kurihara et al. 1998; Wu et al. 2000) and the Weather Research and Forecasting model (WRF, Skamarock et al. 2005), are also discussed. Note that the CWB global model is not used due to the problem with its tracking TCs.

## 2. Background of NOAA Hurricane Surveillance

In 1982, HRD began research flights to explore possible improvements to numerical tropical cyclone track forecasts that result from the assimilation of dropwindsonde observations made in the data-sparse TC environment. From 1982 to 1996, the crews of NOAA's WP-3D aircraft operated by the Aircraft Operations Center (AOC), made dropwindsonde observations in the environments of TCs for 19 synoptic times. The observations, coupled with the improved modeling and data assimilation, helped the Environmental Modeling Center (EMC) of NCEP to reduce track forecast errors significantly (Burpee et al. 1996; Tuleya and Lord 1997). According to Burpee et al. (1996), the increase of observational data made statistically significant contributions to the operational numerical model forecasts (improvement by 16%-30% for 12-60-h forecasts). Additionally, the data have been used in research, such as identifying beta gyres and their effects on TC motion (Franklin et al. 1996).

These encouraging results led to the development of a new generation of Global Positioning System (GPS) dropwindsondes and the purchase by NOAA of a Gulfstream-IV (G-IV) jet aircraft that flies higher and covers a larger area than a P-3, enabling data to be acquired throughout the troposphere and over a larger geographical area than previously available. Since 1997, the G-IV has made dropwindsonde observations when a TC threatens coastal areas of the U.S. in the Atlantic basin, Hawaii, or southern California. Along with these enhancements, new satellite measurements and improved understanding of the atmosphere have resulted in further reduction in TC track error in the operational NOAA models.

With the use of the GPS dropwindsondes, the accuracy of wind observations is greatly enhanced as compared to previous technology (Hock and Franklin 1999). The first-year result with the G-IV surveillance in 1997 revealed that GPS dropwindsonde observations improved the Geophysical Fluid Dynamics Laboratory (GDFL) track and intensity forecasts by as much as 32% and 20%, respectively, in the period within 48 h of projected landfall (Aberson and Franklin 1999).

Recently, a strategy for identifying potential dropwindsonde release locations (targets) to optimize the likelihood that the additional observations would impact the global model TC track forecasts has been developed (Aberson 2003). This strategy employs estimates of initial condition uncertainty and potential error growth from the NCEP operational global ensemble forecasting system and ensures adequate sampling of the target regions. During 2003, thirteen missions were conducted. The dropwindsonde data improved the 24- and 48-h NCEP global model track forecasts by an average of 18% to 32% through five days. Over the last three years, the missions have improved the critical 36 to 60-h global model track forecasts by more than 20%. These forecast times are critical to issuing watches or warnings to alert the public to the threat of TCs. Some evidence suggests that the dropwindsondes produce larger forecast improvements for strong or rapidly intensifying storms (Aberson, personal communication 2005).

The improvements have increased year by year as the sampling technique has been refined and are approaching the values seen in Burpee et al. (1996). The annual percentage improvements to the NCEP Global Forecast System (GFS) range from 10% to 30% for 5-day track forecasts (Aberson 2004).

## 3. The Model Descriptions

To evaluate the impact of dropwindsonde

data on numerical forecasts, three global models [The NCEP GFS, the FNMOC NOGAPS, and the JMA GSM] and two regional models [NCEP GFDL hurricane model and WRF model] are used. The data from the 10 DOTSTAR missions were assimilated into the global models in real time (the control runs, i.e., GFS-D, NOGAPS-D, and GSM-D[1]). The denial experiments (without the dropwindsonde data, i.e., GFS-N, NOGAPS-N, and GSM-N) are retrospective reruns.

The two regional models (GFDL and WRF) were run with the initial and boundary conditions provided by the GFS-D for the control (i.e., GFDL-D and WRF-D), and by the GFS-N for the denial runs (GFDL-N and WRF-N).

a. NCEP GFS

The NCEP GFS (Surgi et al. 1998) is an operational global data assimilation and model system providing forecasts four times per day. During 2004, the horizontal resolution was spectral triangular 254 (T254) with a Gaussian grid of 768 x 384, or roughly equivalent to 0.5 x 0.5 degree latitude/longitude grid spacing; the vertical coordinate extends from the surface to about 2.7 hPa with 64 unequally spaced sigma levels on a Lorenz grid. The NCEP Global Data Assimilation System (GDAS) is composed of a quality control algorithm, a vortex relocation procedure, an analysis procedure, and the NCEP GFS itself (Aberson, 2003).

b. FNMOC NOGAPS model

NOGAPS (Hogan and Rosmond 1991) is a global forecast system with a spectral representation in the horizontal plane and a finite-difference approximation in the sigma vertical coordinate. The operational NOGAPS has a resolution of T239 with 30 vertical levels. The model top extends to 1 hPa with higher resolutions concentrated near the surface and the top boundaries. The data quality is controlled using the techniques described by Baker (1992). The observations that typically go into the data assimilation system are described by Goerss and Phoebus (1992) and include all of the meteorological data available up to 9 h after the analysis time.

The background used in the NOGAPS data analysis is typically the most recent 6-h forecast valid at the analysis time. NOGAPS, like the GFS, uses a three-dimensional variational (3-D VAR) assimilation scheme on a Gaussian grid.

c. JMA GSM

The JMA GSM has a horizontal resolution on a Gaussian grid of T213 with 40 sigma levels from the surface to 0.4 hPa. (The corresponding transform grids are spaced about 0.5625 degree in both longitude and latitude) The JMA 3D-VAR data assimilation system is run four times a day. Typhoon bogus data are embedded in the first guess fields of surface pressure, temperature, and wind. A more detailed description of the model can be found in JMA's website (http://www.jma.go.jp/JMA_HP/jma/jma-eng/jma-center/nwp/outline-nwp/index.htm).

d. GFDL hurricane model

The GFDL hurricane model is a limited-area gridded model developed specifically for hurricane prediction. It includes 18 sigma levels and uses a horizontal finite-difference method with three nested grids. The two inner grids move to follow the storm, and the resolution of the inner domain is 1/6 degree. The GFDL hurricane model includes convective, radiative and boundary layer parameterizations and has a specialized method for initializing the storm circulation such that the storm circulation in the global analysis is replaced with the sum of an environmental flow and a vortex generating by nudging the fields in a separate run of the model to an idealized vortex based upon a few observed parameters, including the maximum wind, radius of maximum wind and outer wind radii. The environmental flow is the global analysis modified by a filtering technique which removes the hurricane circulation. A more detailed description of the GFDL hurricane model can be found in Kurihara et al. (1993, 1995, 1998).

e. WRF model

The previous four models are all for operational use. The WRF model is a next-generation mesocale numerical weather prediction system designed to cater to both operational forecasting and atmospheric research needs. It features multiple dynamical cores, a 3D-VAR data assimilation system, and a software architecture allowing for computational parallelism and system extensibility (Skamarock et al. 2005). A single mesh with 54 km horizontal resolution (161 x 121 grid points in East-West and North-South) and 31 sigma layers vertical resolution (from the surface to 10 hPa) is used in this study.

---

[1] Only the data from the first five missions reached JMA due to some technical problems in data transmission. Therefore, only the five cases with the dropwindsonde data in GSM are examined.

## 4. Results

### a. Data impact on analyses

Figure 2a shows the difference between the control and denial GFS (GFS-D and GFS-N) 925-250-hPa deep-layer mean (DLM) winds for Typhoon Meari at 1200 UTC 25 September, 2004. Major differences are seen at the dropwindsonde locations, with a maximum difference of about 4 m $s^{-1}$ to the south of Meari where the $4^{th}$ through $7^{th}$ dropwindsondes were released. On the other hand, the difference in DLM wind between the NOGAPS-D and NOGAPS-N (Fig. 2b) is smaller, with a maximum of about 1.5 m $s^{-1}$ to the east of Meari, near the 8th and 9th dropwindsondes. Thus, the largest impact on the analysis is near the dropwindsonde locations in both models. However, the different data assimilation schemes in each model generate different impact patterns. More detailed discussions of these differences are presented in Huang et al. (2006).

### b. Impact of the dropwindsonde data on the typhoon track predictions in global models

(1) NCEP GFS

The impact of the dropwindsonde data on NCEP GFS track forecasts for all ten DOTSTAR missions in 2004 are shown in Table 2. The dropwindsonde data lead to mean track error reductions of up to 27% through 72 h, and an average improvement of 14%. Due to the limited number of cases, only the improvements at 42 and 48 h are statistically significant at the 90% confidence level (paired test with one-sided distribution, Larsen and Marx 1981).

Of the 10 cases, the Typhoon Meari at 1200 UTC 25 September, 2004 has the largest track forecast improvement, and the Typhoon Mindulle case at 1200 UTC 29 June, 2004 has the largest forecast degradation. Figure 3 shows the GFS track forecasts from both the control and denial runs for the Meari case. Both the control and denial runs over-predict westward motion during the first 12 h and has a southward bias through 24 h. These biases lead to less interaction between Meari and an approaching mid-latitude trough, and thus the model cannot predict the recurvature of Meari near Okinawa. Nevertheless, a greatly improved track forecast is provided by the control run as compared to the denial run. The mechanics of this improved forecast is presented in Huang et al. (2006).

For the Mindulle case, neither the control nor the denial run predict the sudden northward swerve of the storm at about 24 h (Fig. 4). The control run has a more westward track than the denial run, substantially degrading the forecast. Further work is needed to investigate why the dropwindsonde data have a negative impact in this particular case.

(2) NOGAPS

A similar comparison has also been done using NOGAPS (Table 2). The average track errors of NOGAPS are generally much larger than those from the GFS. The dropwindsonde data contribute to a modest improvement in NOGAPS track predictions, though only the 6-h forecast differences are statistically significant at the 90% confidence level.

(3) JMA GSM

Due to some since-resolved technical problems in data transmission, the JMA only received the dropwindsonde data for the first five cases of 2004, and only these five cases are examined. The dropwindsonde data have a substantial positive impact on the track forecasts through 72 h (Table 2), and the average improvement during the first 72 h is 19%. Due to the limited number of cases, only the forecasts at 12, 18, 30 and 54 h are statistically significant at the 90% confidence level.

(4) The model ensemble mean

The ensemble mean of various model forecasts (Burpee et al. 1996; Zhang and Krishnamurti 1997; Goerss 2000) is frequently used in track forecast and is also a very convenient reference for typhoon forecasters. The ensemble mean of the three global models is calculated both with and without the dropwindsonde data to assess their impact. The impact from the dropwindsonde data is larger in the ensemble mean than in each individual model, as reported in Burpee et al. (1996), and many of the forecasts are statistically significant at the 90 % confidence level.

Figure 5 shows scatter diagrams and the (least square root) fit lines of all forecast errors (from 6 to 72 h) for both the control and denial experiments of the GFS, NOGAPS, GSM and the ENS (three-model ensemble), respectively. Most of the points, as well as the regression line, are located to the upper left of the diagonal line, indicating that the model forecasts with the dropwindsonde data generally have smaller errors than the denial runs, especially for points with large track errors. In addition, Fig. 5d clearly indicates a further enhancement of the positive impact by ENS with more points shifted to the upper-left side of the plot. Further, the regression line for the ENS is shifted to the left of, and has a larger slope than, the lines from the constituent models.

### b. Impact of the dropwindsonde data to the regional models

(1) GFDL hurricane model

The impacts of the dropwindsonde data on the GFDL hurricane and WRF mesoscale models are shown in Table 2. In the first 48 h, the impact of the dropwindsonde data on the GFDL hurricane model forecasts is generally negative, though none of the differences are significant. The impact of the drowindsonde data becomes positive by 48 h, with a substantial improvement of 15-25 % thereafter; the 72-h improvement is statistically significant. The average track error reduction in the GFDL hurricane model with the use of the dropwindsonde data is an insignificant 3%. Note that errors in GFDL models are smaller than the other models which could be one reason for forecast degradation.

Like results in the GFS model, the dropwindsonde data has the most positive impact on the track prediction of Typhoon Meari (Fig. 6). In the control run, the model forecasts the interaction of an approaching mid-latitude trough very well, and the recurvature point of Meari is very close to that indicated in the best track of JTWC, though the eastward translational speed is slightly underestimated afterwards. The track error is reduced to a large extent due to the assimilation of the dropwindsonde data, and the GFDL hurricane model provides the best Meari forecast among all models used in this study.

On the other hand, Typhoon Megi is the case in which the dropwindsonde data has the largest negative impact on the GFDL model (Fig. 7). The track from the control run predicts too much eastward motion, thus leading to a track error of about 200 km at 48 h. To understand why the dropwindsonde data generally degrades the GFDL model forecasts, the DLM wind from the dropwindsonde data and the GFDL-N and GFDL-D DLM wind analysis are compared (Figs. 8a, b). The DLM wind difference between the dropsindsondes and the control run is very small, but the maximum DLM wind difference between dropwindsonde soundings and the model analysis interpolated to the sounding locations is to the east of Megi (14.8 and 14.2 m $s^{-1}$ for GFDL-N and GFDL-D, respectively). The root mean square error (RMSE) of the DLM wind different among the 16 soundings is 6.7 (6.8) m $s^{-1}$ for GFDL-N (GFDL-D). A similar comparison is also performed with the GFS (Figs. 8c, d). The maximum and the RMSE DLM wind difference in GFS-D is much smaller than that in GFS-N (the maximum RMSE DLM difference is 4.7 (2.0) m $s^{-1}$ in GFS-D and 11.3 (5.4) m $s^{-1}$ in GFS-N).

This indicates that the dropwindsonde information does not seem to be affecting the initial condition of the GFDL hurricane model, thus lessening any forecast impact. This result appears consistent with the recent hurricane surveillance program in the western Atlantic conducted by NOAA (Aberson 2003; Aberson and Etherton 2006). An optimal way of appropriately combining the dropwindsonde data with the GFDL vortex is needed in order to improve the impact of the dropwindsonde data, such as the method suggested in Chou and Wu. (2006).

(2) WRF model

The impact of the dropwindsonde data on the WRF model is shown in Table 2. The dropwindsonde data reduce the track error modestly within the first 72 h, and this result is similar to that of the GFS (Table 2). This consistent result is not surprising since the initial and boundary conditions are directly interpolated from the forecast of the appropriate GFS run. Moreover, as a second set of runs in WRF, the dropwindsonde data are also assimilated directly into the WRF model using its 3D-VAR system (Baker et al. 2004), and the overall impact is roughly the same (not shown). A detailed investigation on how different data assimilation schemes affect the impact of data in mesoscale models (MM5 and WRF) is presented in Huang et al. (2006).

## 5. Conclusions

Since 2003, DOTSTAR has successfully made routine surveillance observations for tropical cyclones within range of the Astra jet over the western North Pacific. Throughout 2005, DOTSTAR has successfully completed 19 missions in 15 typhoons and deployed 313 dropwindsondes. Similar runs for the cases during the 2005 season have not yet been completed. Five models (4 operational and 1 research models) were used to evaluate the impact of dropwindsonde data on TC track forecasts during 2004. All models, except the

GFDL hurricane model, show positive impact from the dropwindsonde data on tropical cyclone track forecasts. In the first 72 h, the mean track error reductions in three operational global models, NCEP GFS, NOGAPS and JMA GSM, are about 14, 14, and 19%, respectively, and the mean track error reduction of the ensemble of the three global models is 22%. The track error reduction in the Weather Research and Forecasting (WRF) model in which the initial conditions are directly interpolated from the operational GFS analysis is 16%. Only very little mean track improvement (3%) is shown in the GFDL model, probably because the dropwindsonde data information is affected by the model's vortex initialization scheme.

Further research on the impact of dropwindsonde data on numerical models, and on optimal deployment strategies for the data, is ongoing. A new method of identifying sensitive areas to target observations for tropical cyclone prediction based on the adjoint model has been proposed (Wu et al. 2006). Moreover, a detailed physical examination of targeted dropwindsonde and of data assimilation schemes for the Meari and Conson cases is ongoing (Huang et al. 2006). In addition, the optimal combination of dropwindsonde data and bogus vortices in the model initializations is also proposed (Chou and Wu 2006).

DOTSTAR surveillance missions are planned through 2008 and are being coordinated with the THORPEX Pacific Area Regional Campaign in 2008 (Thorpe and Shapiro, personal communication 2005). As the DOTSTAR research team continues to gather important data and gain valuable experience, future typhoon observations will reach full maturity, enabling significant progress in both academic research and typhoon forecasting. It is hoped that DOTSTAR will shed light on typhoon dynamics, enhance typhoon track forecast accuracy, place Taiwan at the forefront of international typhoon research, and make a significant contribution to the study of typhoons in the northwestern Pacific and East Asia region.

**ACKNOWLEDGEMENTS**

The work is supported through the National Science Council of Taiwan by Grants NSC92-2119-M-002-009-AP1 and NSC93-2119-M-002-013-AP1. The authors wish to thank J.-S. Hong, T.-.J. Yeh, T.-Z. Fong, D.-S. Chen, and W.-M. Chen at CWB for their helpful collaborations. And Mr. Shibiori at JMA for his reruns of the denial experiment of JMA GSM model. The GFS and GFDL runs were made on the NOAA Central Computer.

**REFERENCES**

Aberson, S. D., and J. L. Franklin, 1999: Impact on hurricane track and intensity forecasts of GPS dropwindsonde observations from the first-season flights of the NOAA Gulfstream-IV jet aircraft. *Bull. Amer. Meteor. Soc.*, **80**, 421–427.

______, 2003: Targeted observations to improve operational tropical cyclone track forecast guidance. *Mon. Wea. Rev.*, 131, 1613–1628.

______, and C. R. Sampson, 2003: On the predictability of tropical cyclone tracks in the northwest Pacific basin. *Mon. Wea. Rev.*, **131**, 1491–1497.

______, 2004: The G-IV Surveillance Era, Targeting, and Ensemble Forecasts (1997-Present), Preprint, 26th Conf. on Hurricanes and Tropical Meteorology, Miami, Amer. Meteor. Soc., 236–237.

______, and B. J. Etherton, 2006: Targeting and data assimilation studies during Hurricane Humberto (2001). *J. Atmos. Sci.*, **63**, 175–186.

Barker, D. M., W. Huang, Y.-R. Guo, A. J. Bourgeois, and Q. N. Xiao, 2004: A three-dimensional variational data assimilation system for MM5: Implementation and initial results. *Mon. Wea. Rev.*, **131**, 897–914.

Baker, N. L., 1992: Quality control for the Navy operational atmospheric data base. *Wea. Forecasting*, **7**, 250–261.

Burpee, R. W., S. D. Aberson, J. L. Franklin, S. J. Lord, and R. E. Tuleya, 1996: The Impact of Omega Dropwindsondes on Operational Hurricane Track Forecast Models. *Bull. Amer. Meteor. Soc.*, **77**, 925–933

Chou, K.-H., and C.-C. Wu, 2006: The optimal combination of the bogused vortex and the dropwindsonde data for typhoon initialization in a mesoscale model. To be submitted to Geophys. Res. Lett.

Goerss, J. S., and P. A. Phoebus, 1992: The Navy's operational atmospheric analysis. *Wea. Forecasting*, **7**, 232–249.

______, 2000: Tropical cyclone track forecasts using an ensemble of dynamical models. *Mon. Wea. Rev*., **128**, 1187-1193.

Franklin, K. L., S. E. Feuer, J. Kaplan, and S. D. Aberson, 1996: Tropical Cyclone Motion and Surrounding Flow Relationships: Searching for Beta Gyres in Omega Dropwindsonde Datasets. *Mon. Wea. Rev.*, **124**, 64–84.

Hock, T. F., and J. L. Franklin, 1999: The NCAR GPS Dropwindsonde. *Bull. Amer. Meteor. Soc.*, **80**, 407–420.

Hogan, T. F., and T.E. Rosmond, 1991: The description of the Navy Operational Global Atmospheric Prediction System's Spectral Forecast *Model. Mon. Wea. Rev.*, **119**, 1786–1815.

Huang, W. P., C.-C. Wu, P.-H. Lin, and K.-H. Chou, 2006: The Impact of the Dropwindsonde Data from DOTSTAR on the Prediction of Typhoon Conson (2004) in Numerical Models. Preprint, 27th Conf. on Hurricanes and Tropical Meteorology, Miami, Amer. Meteor. Soc.

Kurihara, Y., M. A. Bender, and R. J. Ross, 1993: An initialization scheme of hurricane models by vortex specification. *Mon. Wea. Rev.*, **121**, 2030–2045.

______, M. A. Bender, R. E. Tuleya, and R. J. Ross, 1995: Improvements in the GFDL hurricane prediction system. *Mon. Wea. Rev.*, **123**, 2791–2801.

______, M. A. Bender, R. E. Tuleya, and R. J. Ross, 1998: The GFDL hurricane prediction system and its performance in the 1995 hurricane season. *Mon. Wea. Rev*., **126**, 1306–1322.

Larsen, R. J., and M. L. Marx, 1981: An introduction to mathematical statistics and its applications. Prentice-Hall, Inc., 530pp.

Skamarock, W. C., J. B. Klemp, J. Dudhia, D. O. Gill, D. M. Barker, W. Wang, J. G. Powers, 2005: A description of the advanced research WRF version 2. NCAR/TN-468+STR., National Center for Atmospheric Research, Boulder, Colorado, USA.

Surgi, N., H.-L. Pan, and S. J. Lord, 1998: Improvement of the NCEP global model over the Tropics: An evaluation of model performance during the 1995 hurricane season. *Mon. Wea. Rev.*, **126**, 1287–1305.

Tuleya, R. E., and S. J. Lord, 1997: The impact of dropwindsonde data on GFDL Hurricane model forecasts using global analyses. *Wea. Forecasting*, **12**, 307–323.

Wu, C.-C., M. Bender, and Y. Kurihara, 2000: Typhoon forecasts with the GFDL hurricane model: Forecast skill and comparison of predictions using AVN and NOGAPS global analyses. *J. Meteor. Soc. Japan*, **78**, 777–788.

______, and Coauthors, 2005: Dropsonde Observations for Typhoon Surveillance near the Taiwan Region (DOTSTAR): An overview. *Bull. Amer. Meteor. Soc.*, **86**, 787-790.

______, J.-H. Chen, P.-H. Lin, and K.-H. Chou, 2006a: Targeted observations of tropical cyclone movement based on the adjoint-derived sensitivity steering vector. Submitted to *J. Atmos. Sci.*

______. K.-H. Chou, P.-H. Lin, S. Aberson, M. Peng, and T. Nakazawa, 2006b: The impact of dropsonde data on typhoon track forecasts in DOTSTAR. Submitted to *Bull. Amer. Meteor. Soc*.

Z. Zhang and T. N. Krishnamurti, 1997: Ensemble Forecasting of Hurricane Tracks. *Bull. Amer. Meteor. Soc.*, **78**, 2785–2795.

Table 1. DOTSTAR synoptic surveillance missions conducted in 2004. The initial position and intensity are from the JTWC best-track, and the intensity is indicated as TY for typhoon or TS for tropical storm. The model evaluation column lists the model used for assessing the impact of the dropwindsonde observations on the numerical forecasts. A is the NCEP GFS, N is NOGAPS, J is JMA, G is GFDL, and W is WRF model.

| No. of mission | Typhoon name | Position | Intensity (m $s^{-1}$) /Strength of TC | Observed time | No. of dropsondes | Model evaluation |
|---|---|---|---|---|---|---|
| 1 | Nida | 15.2°N, 123.7°E | 70.2/TY | 12Z 17 May 2004 | 15 | A/N/J/G/W |
| 2 | Conson | 19.9°N, 120.1°E | 46.8/TY | 12Z 08 Jun 2004 | 16 | A/N/J/G/W |
| 3 | Mindulle | 17.4°N, 127.0°E | 39.0/TY | 12Z 27 Jun 2004 | 16 | A/N/J/G/W |
| 4 | Mindulle | 18.6°N, 125.0°E | 59.8/TY | 12Z 28 Jun 2004 | 16 | A/N/J/G/W |
| 5 | Mindulle | 18.9°N, 123.1°E | 65.0/TY | 12Z 29 Jun 2004 | 14 | A/N/J/G/W |
| 6 | Megi | 19.8°N, 129.8°E | 20.8/TS | 12Z 16 Aug 2004 | 16 | A/N/G/W |
| 7 | Aere | 23.8°N, 125.0°E | 33.8/TY | 12Z 23 Aug 2004 | 18 | A/N/G/W |
| 8 | Meari | 24.5°N, 129.0°E | 57.2/TY | 12Z 25 Sep 2004 | 17 | A/N/G/W |
| 9 | Nockten | 21.7°N, 123.2°E | 33.8/TY | 12Z 24 Oct 2004 | 13 | A/N/G/W |
| 10 | Nanmadol | 17.9°N, 119.0°E | 49.4/TY | 00Z 03 Dec 2004 | 14 | A/N/G/W |

Table 2. Track forecast verification from all models through 72 h. Forecast times in which the forecast error differences are statistically significant at the 90% confidence level are shown in bold. The "Improvement" indicates the difference (in both km and %) between the control and the denial run, with positive (negative) values representing improved (degraded) track forecasts with the assimilation of the dropwindsonde data.

| Model | Track position error | **6** | **12** | **18** | **24** | **30** | **36** | **42** | **48** | **54** | **60** | **66** | **72** | **mean** |
|---|---|---|---|---|---|---|---|---|---|---|---|---|---|---|
| NCEP GFS | GFS-N (km) | 52 | 76 | 98 | 133 | 167 | 171 | **212** | **246** | 232 | 246 | 313 | 294 | 187 |
| | GFS-D (km) | 49 | 61 | 85 | 122 | 124 | 130 | **145** | **181** | 223 | 260 | 300 | 241 | 160 |
| | Improvement (km) | 2 | 16 | 13 | 11 | 43 | 42 | **67** | **65** | 9 | -13 | 13 | 52 | 27 |
| | Improvement (%) | 5 | 21 | 13 | 9 | 26 | 24 | **32** | **27** | 4 | -5 | 4 | 18 | 14 |
| | Case number | 10 | 10 | 10 | 9 | 9 | 9 | **8** | **8** | 7 | 7 | 7 | 6 | |
| FNMOC NOGAPS | NOGAPS-N (km) | **58** | 95 | 131 | 167 | 218 | 253 | 281 | 367 | 445 | 527 | 624 | 501 | 306 |
| | NOGAPS-D (km) | **50** | 81 | 115 | 154 | 197 | 232 | 276 | 344 | 384 | 410 | 479 | 437 | 263 |
| | Improvement (km) | **8** | 14 | 17 | 12 | 21 | 21 | 5 | 23 | 61 | 117 | 146 | 65 | 43 |
| | Improvement (%) | **14** | 15 | 13 | 7 | 10 | 8 | 2 | 6 | 14 | 22 | 23 | 13 | 14 |
| | Case number | **10** | 10 | 10 | 9 | 9 | 9 | 8 | 8 | 8 | 8 | 8 | 7 | |
| JMA GSM | GSM-N (km) | 46 | **80** | **114** | 151 | **203** | 223 | 269 | 355 | **411** | 460 | 590 | 405 | 276 |
| | GSM-D (km) | 38 | **55** | **95** | 114 | **135** | 180 | 212 | 279 | **330** | 393 | 486 | 349 | 222 |
| | Improvement (km) | 9 | **25** | **19** | 37 | **68** | 43 | 57 | 76 | **81** | 67 | 104 | 55 | 53 |
| | Improvement (%) | 19 | **32** | **17** | 25 | **33** | 19 | 21 | 21 | **20** | 14 | 18 | 14 | 19 |
| | Case number | 5 | **5** | **5** | 5 | **5** | 5 | 5 | 5 | **5** | 5 | 5 | 4 | |
| Ensemble Mean | ENS-N (km) | **45** | **67** | 87 | 114 | **150** | 166 | 200 | 267 | 338 | **411** | **528** | 499 | 239 |
| | ENS-D (km) | **38** | **50** | 72 | 97 | **113** | 134 | 170 | 224 | 283 | **320** | **393** | 359 | 188 |
| | Improvement (km) | **8** | **17** | 15 | 17 | **38** | 32 | 30 | 43 | 56 | **91** | **135** | 140 | 52 |
| | Improvement (%) | **17** | **25** | 17 | 15 | **25** | 19 | 15 | 16 | 16 | **22** | **26** | 28 | 22 |
| | Case number | **10** | **10** | 10 | 9 | **9** | 9 | 8 | 8 | 8 | **8** | **8** | 7 | |
| GFDL | GFDL-N (km) | 28 | 53 | 76 | 92 | 132 | 163 | 164 | 209 | 243 | 276 | 333 | **270** | 170 |
| | GFDL-D (km) | 27 | 55 | 88 | 112 | 145 | 180 | 198 | 226 | 227 | 237 | 287 | **203** | 165 |
| | Improvement (km) | 1 | 0 | -11 | -18 | -12 | -16 | -32 | -16 | 16 | 39 | 46 | **67** | 4 |
| | Improvement (%) | 4 | -2 | -15 | -20 | -9 | -9 | -19 | -7 | 6 | 14 | 14 | **25** | 3 |
| | Case number | 10 | 10 | 10 | 9 | 9 | 9 | 8 | 8 | 8 | 8 | 8 | **7** | |
| WRF | WRF-N (km) | 54 | 91 | 125 | 154 | 185 | 218 | 292 | 212 | 253 | 260 | 301 | 336 | 207 |
| | WRF-D (km) | 54 | 69 | 96 | 119 | 144 | 171 | 207 | 192 | 222 | 241 | 267 | 306 | 174 |
| | Improvement (km) | 0 | 21 | 30 | 35 | 41 | 47 | 85 | 20 | 31 | 19 | 34 | 30 | 33 |
| | Improvement (%) | 0 | 24 | 24 | 23 | 22 | 22 | 29 | 9 | 12 | 7 | 11 | 9 | 16 |
| | Case number | 10 | 10 | 10 | 9 | 9 | 9 | 8 | 7 | 7 | 6 | 6 | 6 | |

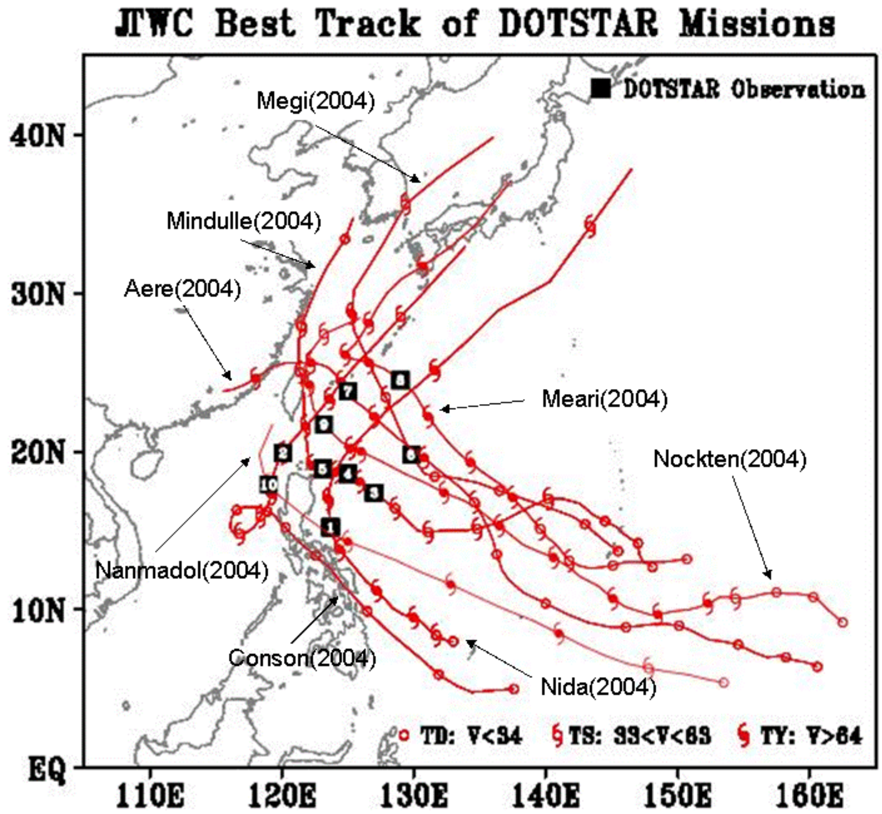


Fig. 1. Locations of the 10 missions conducted in 2004, and the tracks (every 24 h) of the typhoons in which missions were conducted. The number within the square represents the mission.

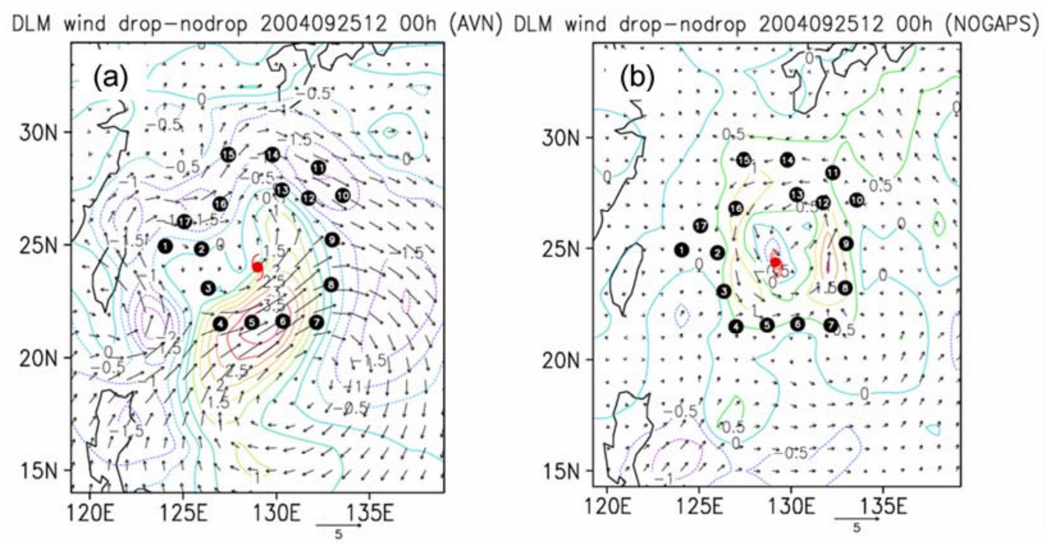


Fig. 2. The deep-layer-mean (925-250-hPa) wind (shaded) and asymmetric wind (vector) differences between analyses with and without assimilation of the dropwindsonde data in (a) NCEP GFS and (b) FNMOC NOGAPS. The black dots indicate the location and order of the dropwindsonde data being assimilated.

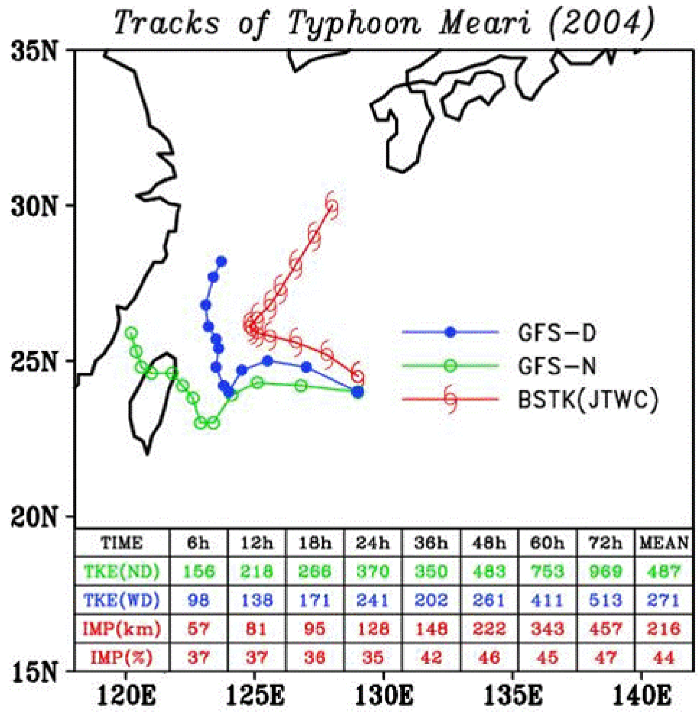


| TIME | 6h | 12h | 18h | 24h | 36h | 48h | 60h | 72h | MEAN |
|---|---|---|---|---|---|---|---|---|---|
| TKE(ND) | 156 | 218 | 266 | 370 | 350 | 483 | 753 | 969 | 487 |
| TKE(WD) | 98 | 138 | 171 | 241 | 202 | 261 | 411 | 513 | 271 |
| IMP(km) | 57 | 81 | 95 | 128 | 148 | 222 | 343 | 457 | 216 |
| IMP(%) | 37 | 37 | 36 | 35 | 42 | 46 | 45 | 47 | 44 |

Fig. 3. The JTWC best track (typhoon symbols), the GFS-N (circles) and GFS-D (dots) forecast tracks of Typhoon Meari initialized at 1200 UTC 25 September, 2004. Track errors are shown in the bottom of the figure. TKE is the track error (km) and IMP is the track error improvement (km and %).

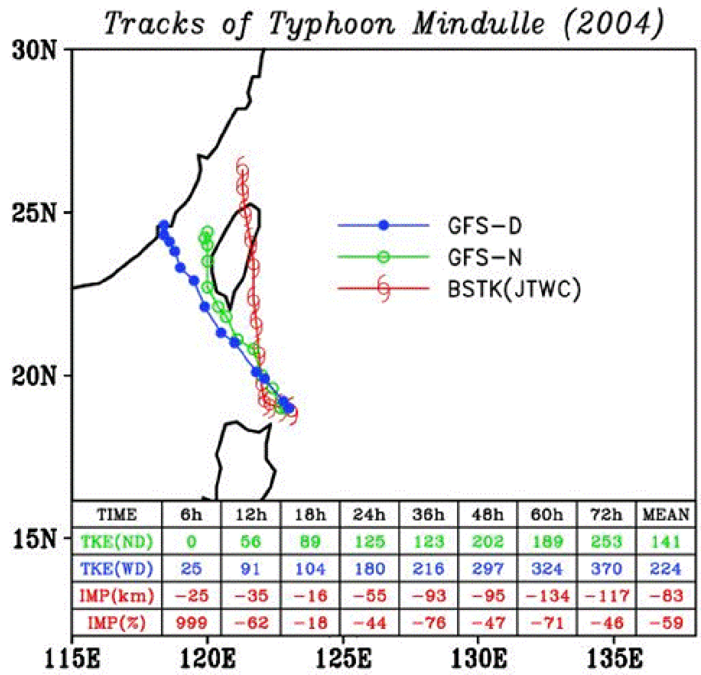


| TIME | 6h | 12h | 18h | 24h | 36h | 48h | 60h | 72h | MEAN |
|---|---|---|---|---|---|---|---|---|---|
| TKE(ND) | 0 | 56 | 89 | 125 | 123 | 202 | 189 | 253 | 141 |
| TKE(WD) | 25 | 91 | 104 | 180 | 216 | 297 | 324 | 370 | 224 |
| IMP(km) | −25 | −35 | −16 | −55 | −93 | −95 | −134 | −117 | −83 |
| IMP(%) | 999 | −62 | −18 | −44 | −76 | −47 | −71 | −46 | −59 |

Fig. 4. As in Fig. 3, but for Typhoon Mindulle initialized at 1200 UTC 29 June, 2004.

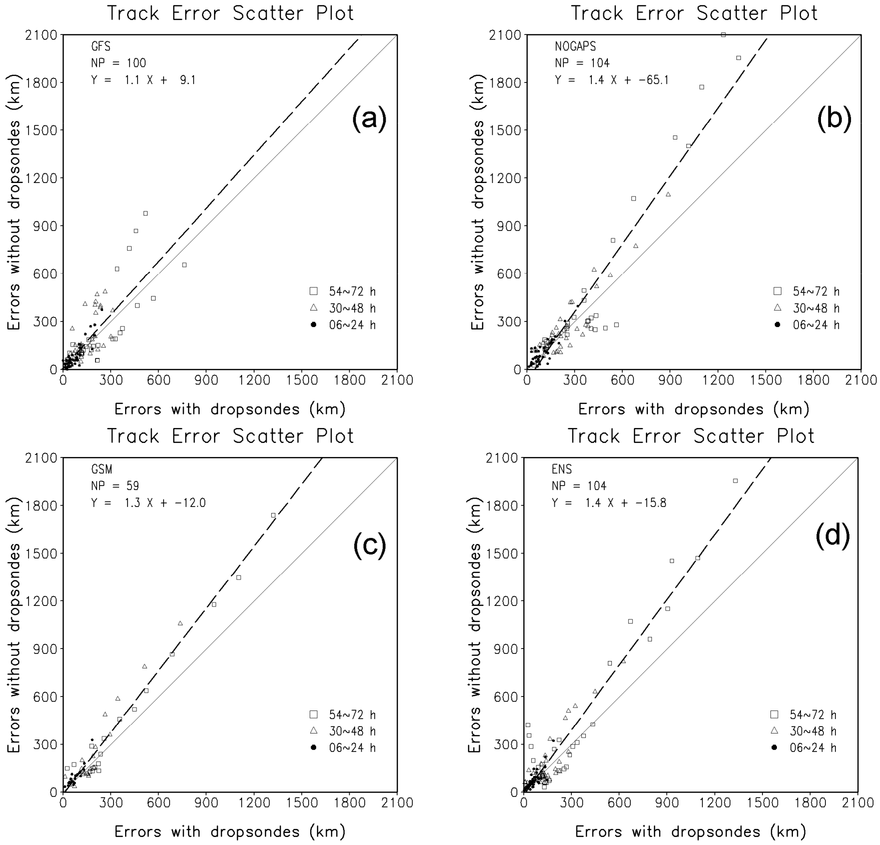


Fig. 5. Scatter plots of model track forecast errors with and without dropwindsonde data during the first 72 h, every 6 h. (a) GFS, (b) NOGAPS, (c) GSM and (d) global model ensemble mean forecasts. The regression line and equation are shown. NP is the number of the points in each figure.

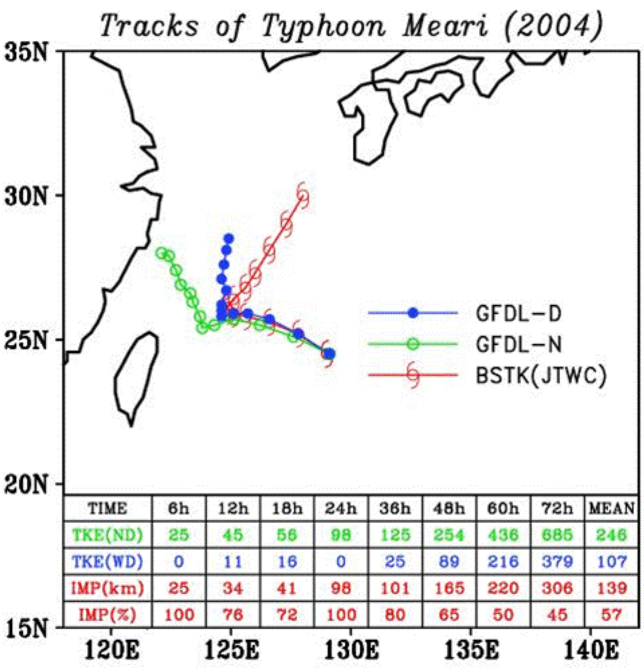


| TIME | 6h | 12h | 18h | 24h | 36h | 48h | 60h | 72h | MEAN |
|---|---|---|---|---|---|---|---|---|---|
| TKE(ND) | 25 | 45 | 56 | 98 | 125 | 254 | 436 | 685 | 246 |
| TKE(WD) | 0 | 11 | 16 | 0 | 25 | 89 | 216 | 379 | 107 |
| IMP(km) | 25 | 34 | 41 | 98 | 101 | 165 | 220 | 306 | 139 |
| IMP(%) | 100 | 76 | 72 | 100 | 80 | 65 | 50 | 45 | 57 |

Fig. 6. As in Fig. 3, but for GFDL and Typhoon Meari initialized at 1200 UTC 25 September, 2004.

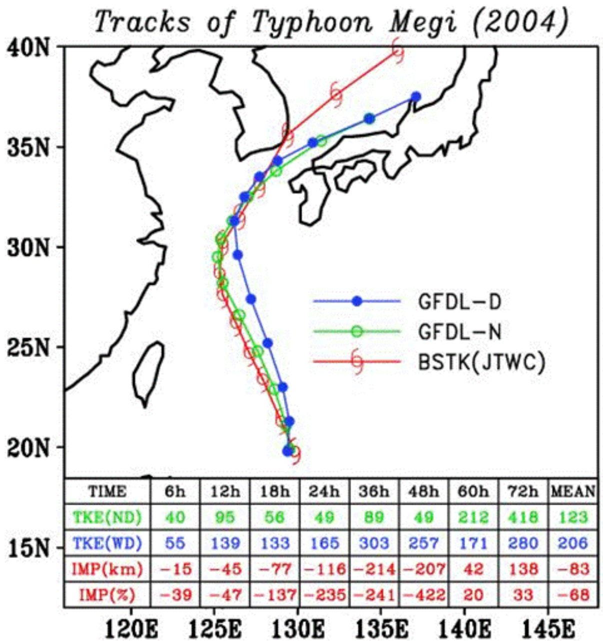


| TIME | 6h | 12h | 18h | 24h | 36h | 48h | 60h | 72h | MEAN |
|---|---|---|---|---|---|---|---|---|---|
| TKE(ND) | 40 | 95 | 56 | 49 | 89 | 49 | 212 | 418 | 123 |
| TKE(WD) | 55 | 139 | 133 | 165 | 303 | 257 | 171 | 280 | 206 |
| IMP(km) | −15 | −45 | −77 | −116 | −214 | −207 | 42 | 138 | −83 |
| IMP(%) | −39 | −47 | −137 | −235 | −241 | −422 | 20 | 33 | −68 |

Fig. 7. As in Fig. 3, but for Typhoon Megi initialized at 1200 UTC 16 August, 2004.

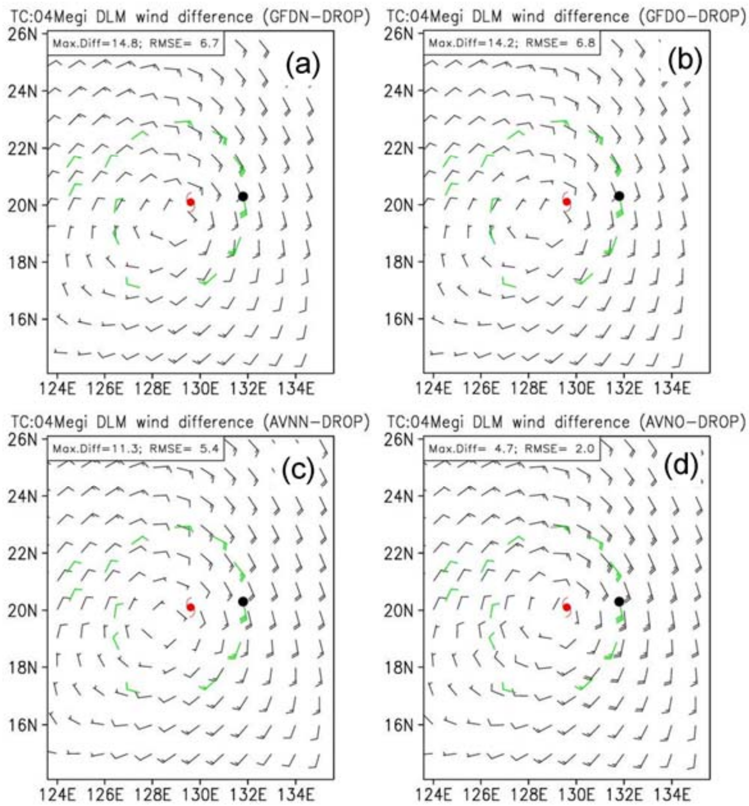


Fig. 8. The deep-layer-mean (925-250-hPa) wind comparison of the sounding from dropwindsonde (green wind barb) and the model analysis (black wind barb, interpolated to the location of the sounding): (a) GFDL-N, (b) GFDL-D, (c) GSM-N and (d) GFDL-D. The dot point means the location where the biggest DLM difference appears. The values draw on the upper left corner show the value of the maximum DLM difference and the root mean square error (RMSE) among all dropwindsondes.